

The branchial arches and HGF are growth-promoting and chemoattractant for cranial motor axons

Adele Caton^{1,*}, Adam Hacker^{1,*}, Arifa Naeem¹, Jean Livet², Flavio Maina³, Friedhelm Blatt⁴, Rüdiger Klein³, Carmen Birchmeier⁴ and Sarah Guthrie^{1,‡}

¹Centre for Developmental Neurobiology, 4th Floor New Hunt's House, King's College, Guy's Campus, London SE1 9RT, UK

²INSERM Unité 382, IBDM (CNRS-INSERM-Université de la Méditerranée), Campus de Luminy, 13288 Marseille Cedex 09, France

³Cell Regulation Programme, European Molecular Biology Laboratory, 69117, Heidelberg, Germany

⁴Max-Delbrück-Centrum für Molekulare Medizin, Robert-Rossle-Strasse 10, 13122 Berlin, Germany

*These authors contributed equally to the work

‡Author for correspondence (e-mail: sarah.guthrie@kcl.ac.uk)

Accepted 26 January; published on WWW 21 March 2000

SUMMARY

During development, cranial motor neurons extend their axons along distinct pathways into the periphery. For example, branchiomotor axons extend dorsally to leave the hindbrain via large dorsal exit points. They then grow in association with sensory ganglia, to their targets, the muscles of the branchial arches. We have investigated the possibility that pathway tissues might secrete diffusible chemorepellents or chemoattractants that guide cranial motor axons, using co-cultures in collagen gels. We found that explants of dorsal neural tube or hindbrain roof plate chemorepelled cranial motor axons, while explants of cranial sensory ganglia were weakly chemoattractive. Explants of branchial arch mesenchyme were strongly growth-promoting and chemoattractive for cranial motor axons. Enhanced and oriented axon outgrowth was also elicited by beads loaded with Hepatocyte Growth Factor

(HGF); antibodies to this protein largely blocked the outgrowth and orientation effects of the branchial arch on motor axons. *HGF* was expressed in the branchial arches, whilst *Met*, which encodes an HGF receptor, was expressed by subpopulations of cranial motor neurons. Mice with targeted disruptions of *HGF* or *Met* showed defects in the navigation of hypoglossal motor axons into the branchial region. Branchial arch tissue may thus act as a target-derived factor that guides motor axons during development. This influence is likely to be mediated partly by Hepatocyte Growth Factor, although a component of branchial arch-mediated growth promotion and chemoattraction was not blocked by anti-HGF antibodies.

Key words: Cranial motor axons, Branchial arches, Chemoattraction, Hepatocyte Growth Factor, Rat embryo

INTRODUCTION

During neural development, axons navigate with precision to their targets. This process depends on the exact deployment in space and time of molecules that bind to axonal surface receptors. Axon guidance cues may act in a contact-mediated fashion, or via diffusion, and may display positive or negative interactions (reviewed by Tessier-Lavigne and Goodman, 1996). The current balance of evidence favours the idea that directional information is imparted to growth cones by diffusible molecules which are chemoattractants, luring growth cones towards their targets, or chemorepellents, deflecting them from inappropriate territory. Examples of molecules mediating these effects are members of the Netrin and Semaphorin families of guidance molecules; individual molecules within these families may possess dual function (reviewed by Varela-Echavarría and Guthrie, 1997; Bagnard et al., 1998). In addition, membrane-associated molecules such as the Ephrins and their Eph receptors play extensive roles in axon guidance (reviewed by O'Leary and Wilkinson, 1999).

We have investigated the possible influence of diffusible molecules on axon pathfinding of subpopulations of cranial motor neurons in the rat embryo. Within the midbrain and hindbrain, motor neurons form a ventral column in the basal plate on either side of the floor plate. Cranial motor neurons may be categorised as somatic motor (SM), branchiomotor (BM) or visceral motor (VM), based on the position of their cell bodies within the dorsoventral and mediolateral axes, their axonal trajectories, and eventual synaptic targets. More than one of these neuronal classes may co-exist within a single nucleus or rhombomere. Cranial motor nuclei lie in the midbrain (oculomotor nucleus, III – SM) and in the hindbrain where they occupy single segments (rhombomeres) or pairs of rhombomeres (Fig. 1A; Lumsden and Keynes, 1989; Gilland and Baker, 1993). Within the hindbrain, the SM nuclei of the trochlear (IV), abducens (VI) and hypoglossal (XII) lie within rhombomere 1 (r1), r5 and r8 respectively. Of the BM and VM nuclei the trigeminal (V – BM) lies in r2/3, the facial (VII – BM/VM) in r4/r5, the glossopharyngeal (IX – BM/VM) in r6 and the vagus (X – BM/VM) and cranial accessory (XI – BM) in r7/r8.

Initially, motor axons grow away from the midline floor plate, before segregating along either ventral or dorsal pathways. SM axons exit the neural tube ventrally in small groups, with the exception of the trochlear nerve, which exits dorsally (Fig. 1A). BM and VM axons project to large single dorsal exit points within rhombomeres 2, 4, 6 and 7 (Fig. 1A). Motor axons from two adjacent rhombomeres converge on a single exit point; for example the trigeminal nucleus occupies r2 and r3, but all axons exit in r2. Once in the periphery, BM and VM axons grow in association with the cranial sensory ganglia. Then BM axons navigate towards the muscle plates of the branchial arches (Fig. 1C), whilst VM axons grow rostrally towards the parasympathetic ganglia (VM). SM axons project towards extra-ocular or tongue muscles, which are derived from paraxial or prechordal plate mesoderm (extra-ocular muscles) or the occipital somites (tongue muscles).

Among the pathway tissues implicated in axon guidance, the floor plate is known to produce diffusible chemorepellents that exclude motor axons from the midline (Guthrie and Pini, 1995; Tucker et al., 1996). The expression patterns of the chemorepellents Netrin 1 and Semaphorin 3A, together with the chemosensitivity of motor neuron subpopulations to these molecules make them promising candidates to mediate this effect (Kennedy et al., 1994; Colamarino and Tessier-Lavigne, 1995; Püschel et al., 1995; Varela-Echavarría et al., 1997). The exit point also seems to play a role in motor axon guidance since following reversal of rostrocaudal polarity of rhombomere 3 or 5, the majority of axons originating in the reversed rhombomere still grew towards the appropriate exit point (Guthrie and Lumsden, 1992). This suggests that signals from the exit point specific to appropriate motor neuron subsets may predominate over intrinsic polarity cues within the segment.

Candidate tissues producing chemoattractant cues thus include the dorsal neural tube (alar plate) that contains the exit point, and the sensory ganglia (Figure 1C). Possible sources of exit point cues include a late-emigrating population of neural crest cells, which form the interface between the neuroepithelium and the sensory ganglion (Niederländer and Lumsden, 1996). Moreover, the roof plate might be chemoattractive, or might limit motor axons' dorsal trajectories by repulsion, since in the spinal cord BMPs present in the roof plate repel commissural axons (Augsburger et al., 1999). Lastly, the peripheral targets of cranial motor axons such as the muscles of the branchial arches might be the origin of chemoattractant guidance cues. This possibility is supported by the finding that in the trunk, spinal motor axons are attracted by their targets, the somitic sclerotome and the limb buds (Ebens et al., 1996). In this study, limb bud-mediated chemoattraction was attributed to Hepatocyte Growth Factor (HGF), a protein originally identified as a mitogen for hepatocytes and a motility enhancing-factor for epithelial cells (Nakamura et al., 1989; Stoker et al., 1987). HGF influences the growth of a number of neuronal types (reviewed by Maina and Klein, 1999). It is a survival and outgrowth-promoting factor for spinal motor neurons (Ebens et al., 1996; Yamamoto et al., 1997), as well as enhancing the survival and outgrowth of sensory neurons (Maina et al., 1997) and the outgrowth of sympathetic neurons (Maina et al., 1998). These properties make HGF a promising candidate to influence cranial motor axon pathfinding.

We have explored the role of diffusible guidance molecules by culturing tissue explants containing subsets of cranial motor

neurons together with pathway tissues in collagen gels. Explants containing motor neurons were isolated from the ventral third of the neural tubes of E12 rat embryos at midbrain, hindbrain or spinal cord levels (Fig. 1B). Tissues selected for co-culture were the dorsal neural tube and the roof plate of the hindbrain, the cranial sensory ganglia, and the branchial arches (Fig. 1D). We tested the possibilities that these tissues might provide diffusible signals that guide cranial motor axons.

MATERIALS AND METHODS

Dissection of embryonic tissues for co-culture

Sprague-Dawley rat embryos were obtained at E12 and E13. Motor neuron-containing explants were dissected using Dispase (Boehringer) and tungsten needles, as described previously (Guthrie and Pini, 1995; Varela-Echavarría et al., 1997). Tissues were washed in Hank's Balanced Salt Solution (HBSS; Gibco) and kept on ice until needed. Midbrain and hindbrain explants were bilateral, encompassing the ventral third of the neuroepithelium on either side of and including the floor plate. Unilateral explants containing SM spinal motor neurons were isolated from the cervical spinal cord (Fig. 1B). Oculomotor explants consisted of the caudal part of the midbrain whilst trochlear explants consisted of the rostral part of r1. Other hindbrain explants contained r2/r3, r4/r5, r6 or r7/r8. For cultures of abducens or hypoglossal neurons labelled from their ventral exit points, r5 or r7/8 explants respectively were used.

Pathway tissues were dissected as shown in Fig. 1D. Dorsal neural tube explants were two rhombomeres long consisting of the dorsal third of the neural tube including the exit points. The explants used were taken from r2/r3 or r4/r5 axial levels. Roof plate explants consisted of the entire roof of the fourth ventricle from a single embryo. Trigeminal ganglia were isolated by making transverse body sections of E12 embryos at trigeminal level and then dissecting the ganglion free of its adjacent tissues. First or second branchial arches were dissected into pieces one third to one half of an arch in size, and the ensheathing ectoderm was removed.

Retrograde labelling of cranial nerves before culture

E12 rat embryos were pinned ventral side up in Sylgard dishes, and the dorsal or ventral nerve roots (Fig. 1A) were transected. Fluorescein dextran crystals (Molecular Probes, Oregon) were diluted in PBS and allowed to dry to a viscous consistency before being applied to the cut ends of the nerves using fine forceps. Embryos were then incubated in Earle's Balanced Salt Solution (Gibco) in a 95% O₂, 5% CO₂ atmosphere for 3 hours to allow retrograde transport of tracer before dissection of tissues.

HGF beads and anti-HGF neutralising antibodies

Heparin-acrylic beads were incubated in a solution of human recombinant HGF (200 µg/ml; R & D Systems) protein or in HBSS alone for 3 hours at room temperature. Beads were then washed several times in HBSS before use as clusters of 5-10 beads as a focal source of HGF in co-cultures. Neutralising antibodies against human HGF (R & D Systems), at 20 µg/ml, were used in selected cultures with HGF-loaded beads. Neutralising antibodies against murine HGF (IW66, kind gift from E. Gherardi) were made up at 20-30 µg/ml and added to the medium in selected cultures at the beginning of the culture period.

Collagen gels and orientation of explants

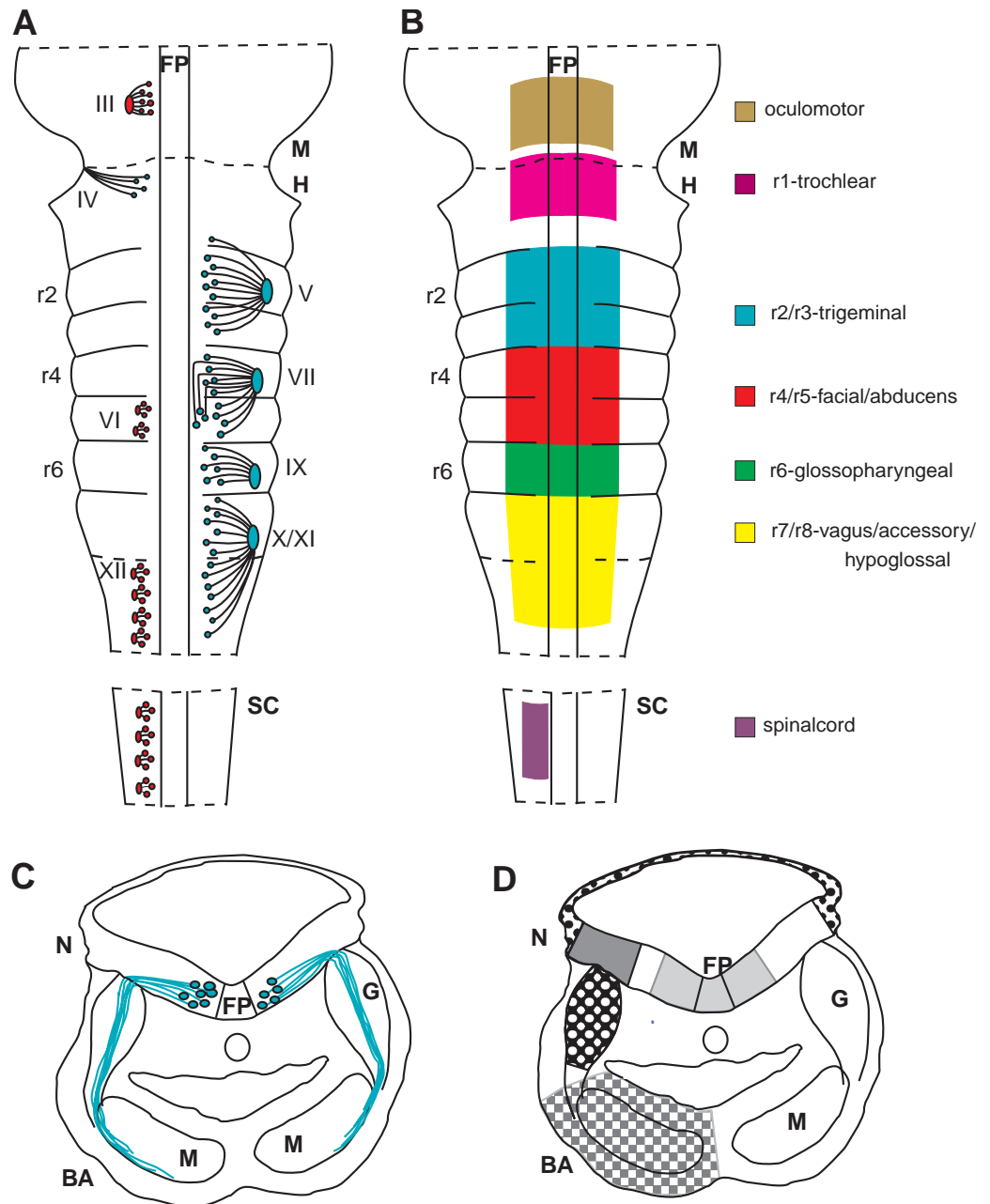
Rat tail collagen was prepared and made into gels as described previously (Guthrie and Lumsden, 1994). Tissue pieces and/or beads were placed in the gels in various combinations, with 100-500 µm separation between the tissues. Tissue pieces were cultured in medium consisting of 75% OptiMEM with GLUTAMAX (Gibco) and 25% F12 (Gibco) supplemented with 5% foetal calf serum, 40 mM glucose and

Fig. 1. Schematic diagrams of hindbrain and surrounding tissues. (A) Schematic diagram of arrangement of motor nuclei in the E12 rat embryo brainstem and spinal cord shown in flat-mount view. Somatic motor neurons are depicted on the left of the diagram and branchiomotor and visceral motor neurons are depicted on the right. Neurons with ventral trajectories are shown in red and those with dorsal trajectories in blue. R2, r4, and r6 show the positions of rhombomeres. FP, floor plate; M, midbrain; H, hindbrain; SC, spinal cord; III, oculomotor nucleus; IV, trochlear nucleus; V, trigeminal nucleus; VI, abducens nucleus; VII, facial nucleus; IX, glossopharyngeal nucleus; X, vagus nucleus; XI, cranial accessory nucleus; XII, hypoglossal nucleus.

(B) Schematic diagram of explants dissected from E12 rat embryo brainstem, shown as a flat mount. Regions are shown by coloured shading, and motor nuclei included in each explant are indicated in the key.

Midbrain and hindbrain explants were all bilateral, including the floor plate. Spinal cord explants were unilateral, not including the floor plate. (C) Schematic diagram of transverse section through the hindbrain and adjacent branchial arches, showing branchiomotor and visceral motor axon pathways (in blue). N, neuroepithelium; FP, floor plate; G, sensory ganglion; BA, branchial arch; M, muscle plate.

(D) Similar transverse section to that in C, showing tissues dissected for co-culture experiments. Light gray, ventral explants containing motor neurons; dark gray, alar plate; black spots, roof plate; white spots, ganglion explant; chequer-board shading, branchial arch.



1% penicillin/streptomycin (Colamarino and Tessier-Lavigne, 1995). All explants dissected from hindbrain levels were bilateral, and were oriented with one lateral (dorsal) side, or in some cases with the rostral/caudal edge, facing the pathway explant. Midbrain explants were also oriented with one lateral edge adjacent to the test explant. Unilateral spinal cord explants grew radially under control conditions, and were oriented at random with respect to cell aggregates. In all cases, the explant border facing the pathway explant was considered as side 1, and the side facing diametrically away was considered as side 2.

Quantitation of axon outgrowth

Semi-quantitative analysis

Axon outgrowth was observed at regular intervals throughout the culture period and semi-quantitative data was obtained by observation

of live cultures under phase contrast immediately before fixation, at 36-40 hours. A graticule with cross hairs was aligned diagonally to the sides of, and centred on, the neural tube explant, and axon outgrowth was judged semi-quantitatively within each quadrant (side) based on the number and the length of axons, on a scale of 0-5. On this scale, 0 represented no outgrowth, whilst 5 represented some hundreds of axons, attaining lengths of 400-500 μm . For examples of this scoring system, see Fig. 2. Blind assessments of outgrowth were made in most experiments, and in co-cultures of branchial arches with and without anti-HGF antibodies.

For each explant, the outgrowth from the side facing towards the target minus the outgrowth from the side facing away from the target was calculated, giving a positive or negative integer that indicated chemoattraction or chemorepulsion respectively. Thus, for explants in

lateral orientation, growth from the lateral sides was counted, whilst for explants co-cultured in rostral/caudal orientation, growth from rostral and caudal sides was counted. For each category of co-culture, the percentage of explants in a particular category on the -5 to $+5$ scale was represented in a bar chart (see Figs 4, 5). If the majority of explants gave a value of 0 this indicates symmetrical outgrowth. If the majority of explants show positive or negative values this indicates chemoattraction or chemorepulsion respectively. These relative values for each explant were pooled and presented as bar charts for each tissue combination. For each explant category, the values obtained were compared with symmetrical outgrowth, using the Wilcoxon test or Mann-Whitney U-test (see Tables 1 and 2). In addition, pairwise comparisons of the distribution of values for explant categories was made where relevant, for example, hindbrain and arch cultures with and without anti-HGF antibodies.

Quantitative analysis

Some gels containing a hindbrain explant cultured alongside a branchial arch, or a hindbrain explant placed with its rostral/caudal border adjacent to an arch explant were analysed by computerised methods. Immunostained explants were photographed and images were scanned into Photoshop. The explant tissue was deleted from the image so that only pixels representing axon outgrowth remained. Cross hairs were placed on the image to denote quadrants containing explant borders facing arch explants, and those facing away. Quadrants were pasted into ImageTool and converted to black and white. For each explant, black pixels were counted in towards and away-facing quadrants and the data recorded in Excel. Subtraction of away-facing values from towards facing values for each explant gave a point of comparison with the semi-quantitative analysis, using the Mann-Whitney U-Test. To present these results graphically, we calculated a ratio for axon outgrowth towards and away from the target explant in each co-culture and then derived a mean for each category. Where this value is 1 it denotes symmetrical outgrowth, whilst a value exceeding 1 shows chemoattraction (see Fig. 6E).

Immunostaining of collagen gels

Some gels were fixed for immunostaining as described previously (Guthrie and Lumsden, 1992; Varela-Echavarría et al., 1997) using monoclonal antibody 2H3 (Developmental Studies Hybridoma Bank) which recognises the 165 kDa neurofilament protein (Dodd et al., 1988). Gels were mounted under propped coverslips in 90% glycerol/10% PBS and photographed using Nomarski optics. For explants in which motor neurons were prelabelled with fluorescein dextran, gels were observed using blue epifluorescence or imaged using a laser-scanning confocal microscope. Counts of fluorescently labelled axons were made from explant quadrants facing towards and away from target explants, to give an indication of chemoattraction or chemorepulsion.

In situ hybridisation of embryos for *HGF*, *Islet 1* and *Met* expression

Whole-mount in situ hybridisation was performed on E11-12 rat embryos or E10-13 mouse embryos, or on E4 chick embryos. The *Islet 1* probe was a 1.5 kb rat fragment kindly provided by T. Jessell. The *Met* probe was transcribed from two mouse *Met* fragments (nucleotides 301-1576 and 1673-2730; GenBank Y00671) subcloned from a *Met* clone provided by E. Audero and C. Ponzetto. The chick and rat *HGF* probes were obtained from C. Stern and T. Braun respectively.

Embryos or dissected brainstems were fixed overnight in 4% paraformaldehyde, 0.1% Tween 20, followed by permeabilisation with ethanol or methanol and proteinase K. Preparations were then postfixed (20 minutes in 4% paraformaldehyde, 0.1% glutaraldehyde, 0.1% Tween 20) and prehybridised for 1 hour at 70°C in 1.3× SSC, 50% formamide, 2% Tween 20, 0.5% Chaps, 5 mM EDTA and 50 µg/ml yeast RNA. Hybridisation was performed overnight with DIG-

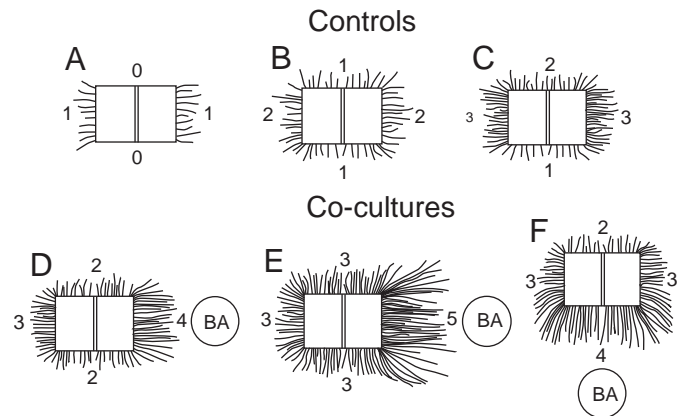


Fig. 2. Diagrammatic representation of the system used for scoring cranial motor axon outgrowth. In each case a graticule with crossing hairs was superimposed on a diagonal relative to the explant (not shown) and the outgrowth from each quadrant was recorded. Examples of different patterns of outgrowth are illustrated for control explants (A-C) and co-cultures with branchial arch explants (D-F) in lateral orientation (D,E) and rostrocaudal orientation (F).

or fluorescein-labelled riboprobes in the same buffer. For the mouse *Met*-specific probe, post-hybridisation washes were followed by RNase A treatment (10 µg/ml in 0.5 M NaCl, 10 mM Tris (pH 7.5) and 0.1% Tween 20, 1 hour at 37°C), and other washes with hybridisation buffer. Embryos were then blocked in maleate buffer containing 20% sheep serum or in PBT (PBS, 0.1% Tween 20) and 10% sheep serum, and incubated overnight at 4°C with AP-conjugated antibody. After extensive washes, the colour reaction was performed using NBT and BCIP (blue) or IBT/BCIP (red). Double in situ hybridisations were performed sequentially using *Islet 1* (red reaction product) and *Met* (blue reaction product).

Analysis of HGF and *Met*^{D/D} mutant mice

The generation of mice carrying targeted disruptions of HGF and *Met* has been described previously (Schmidt et al., 1995; Maina et al., 1996). In *HGF*^{-/-} embryos, exon 2 of the HGF gene encoding part of the protein binding domain essential for receptor binding has been replaced with the neomycin resistance gene (Schmidt et al., 1995). *Met*^{D/D} embryos carry mutations in two tyrosine residues in the *Met* receptor necessary for downstream signal transduction, and manifest defects identical to that in *Met* null mutants (Maina et al., 1996). *HGF*^{-/-} and *Met*^{D/D} E10.5 mouse embryos were fixed overnight at 4°C in Dent's fixative (1:4 DMSO/methanol) and immunostained using anti-NF160 antibody (N-5264; Sigma) as described previously (Maina et al., 1997).

RESULTS

Analysis of cranial motor axon outgrowth in co-cultures with pathway tissues

For hindbrain explants grown alone, motor axon outgrowth occurred from the lateral and from the rostral/caudal borders of the neuroepithelium (Fig. 3A). Based on previous retrograde labelling experiments, it is likely that motor neurons constitute most of the population of differentiated neurons in this region of the neuroepithelium at E12, and extend axons from lateral explant borders as they do in vivo (Guthrie and Pini, 1995; Varela-Echavarría et al., 1997). Straighter, more fasciculated axons which extend from rostral and caudal edges of explants

probably represent axons that form the medial longitudinal tracts *in vivo*. There was some variability in the axon outgrowth observed in control explants (compare Fig. 3A with Fig. 5D).

Most co-culture combinations involved placing pathway tissues laterally, in the region where motor axons would normally emerge. In some cultures, pathway tissues were placed rostral/caudal of the hindbrain explant, since this allowed for the possibility of axons growing directly towards or away from a putative source of guidance cues. The field of axon guidance is fraught with semantic difficulties. Many, but not all axon guidance molecules have been shown both to promote growth and chemoattract, or to inhibit and chemorepel. In our experiments we did see effects of tissues and molecules on the amount of axon growth as well as the direction of guidance. Thus, in experiments with explants placed in lateral orientation, the responses we saw were likely to be a combination of these two aspects; for example branchial arch explants elicited both promotion of growth and chemoattraction. In experiments with explants placed in rostral/caudal orientation, we could analyse directional effects separately. For the purposes of representing these results graphically, however, we have considered that irrespective of explant orientation, greater axon outgrowth towards the pathway tissue than away reflects 'chemoattraction', whereas greater outgrowth away from the pathway tissue than towards reflects 'chemorepulsion' (see Materials and Methods). Please note that these terms are used largely for convenience. Symmetrical outgrowth therefore gives a score of 0 and can readily be compared with asymmetric outgrowth indicative of chemorepulsion (negative values) or chemoattraction (positive values). For control explants, 85.8% grew symmetrically, with 7.1% showing attraction and 7.1% showing repulsion; this distribution is not significantly different from symmetry (Fig. 4A).

Responses of cranial motor axons to the dorsal neural tube and the roof plate

Explants of dorsal neural tube from r2/r3 or r4/r5 axial levels were combined with appropriate or inappropriate motor neuron populations of the trigeminal or facial nucleus levels (r2/r3 or r4/r5 hindbrain explants respectively). In these cultures more explants showed chemorepulsion (44.6%) than showed chemoattraction (14.3%; Fig. 4B). The distribution of these data was significantly different from symmetry, implying that the dorsal neural tube is inhibitory and/or chemorepellent for cranial motor axons, and this was independent of whether combinations of tissues were from the correct or the incorrect axial level (Fig. 4B). These results were surprising, since previous *in vivo* transplantation experiments had indicated that the exit point region might play a chemoattractant role in directing cranial motor axon outgrowth (Guthrie and Lumsden, 1992). However, cells at the exit point that produce chemoattractants may exist in such small numbers that their effect is undetectable in a collagen gel, or these cells may be lost during the tissue preparation. Chemorepulsion by the dorsal neural tube may be explained by the inclusion of tissue dorsal to the exit point which deflects motor axons (see below). Co-cultures with the hindbrain roof plate showed this tissue to be inhibitory and/or chemorepellent for motor neurons at axial levels of r2-8 (Figs 3B, 4B). Roof plate chemorepulsion was observed in 60% of explants and was more pronounced than

that elicited by the dorsal neural tube. *In vivo*, the roof plate may thus act to exclude motor axons from dorsal regions, perhaps via a gradient of inhibitory/chemorepellent molecules that declines from the roof plate to the dorsal neural tube.

Cranial sensory ganglia chemoattract cranial motor axons

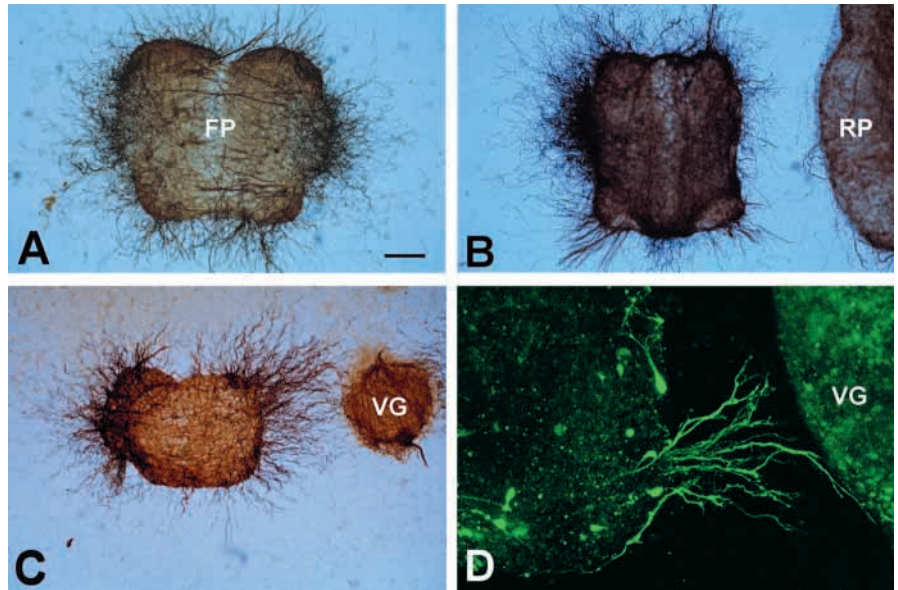
Cranial sensory neurons may be the origin of guidance cues since their axons extend into the hindbrain via entry points which are shared with, or which lie in proximity to motor axon exit points. In co-cultures with a trigeminal ganglion, r2-r8 hindbrain explants showed increased axon outgrowth on the side facing the ganglion and departed significantly from symmetrical outgrowth (Fig. 3C; Table 1). Axons were also seen to turn towards the ganglion explant. Retrograde labelling before culture showed that fluorescently labelled axons of dorsally projecting motor neurons grew towards ganglion explants (Fig. 3D). Both E12 and E13 ganglia were effective, but more explants exhibited increased growth and chemoattraction in combination with E13 than with E12 ganglia (76.3% compared with 49%; Fig. 4D,C). When these co-cultures were immunostained using pan-neuronal antibodies, few neurons were evident within the ganglion, possibly reflecting a lack of trophic factors in the cultures. For this reason we compared sensory neuron viability in co-cultures incubated in medium supplemented with NGF. In these cultures, large numbers of sensory neurons survived and could be immunostained (data not shown). However, motor axon outgrowth from explant borders facing the ganglion was not increased relative to the outgrowth observed in cultures lacking NGF (Fig. 4D). This implies that enhanced motor axon outgrowth and/or chemoattraction in response to ganglia depends on cell types other than sensory neurons, such as Schwann cells or mesenchyme cells (see below).

Branchial arches chemoattract and promote the growth of cranial motor axons

Branchial arches are candidates for the production of axon guidance molecules since they are the targets for BM neurons. Branchial arches consist of an external sheath of ectoderm and endoderm and an internal layer of mesenchymal cells, derived from the paraxial mesoderm and the neural crest (reviewed by Noden, 1988). During development, BM axons grow into the muscle plate which differentiates from the paraxial mesoderm and occupies the core of the arch, but avoid surrounding regions of neural crest-derived mesenchyme (Simon et al., 1994).

When r2-r8 hindbrain explants were placed with their lateral edges facing an arch explant, there was a strong promotion of axon outgrowth. This was reflected in a striking increase in both the number and the length of axons extending from explant borders adjacent to arch explants compared with explant borders facing away (Fig. 5A). This effect was observed over distances of 1-2 mm within the gels (Fig. 5B). Outgrowth patterns were significantly different from symmetrical outgrowth (Fig. 4E; Table 1). 80.4% of explants cultured with arches exhibited more outgrowth towards the arch than away from it. Our observations suggest that the effect of the arch was both chemoattractive and growth-promoting. However, in this study we have concentrated on quantitating the chemoattractive rather than the growth-

Fig. 3. Responses of cranial motor axons to roof plate, and sensory ganglion explants. A-C are co-cultures stained with anti-neurofilament antibodies. D is a confocal image of retrogradely labelled motor axons. (A) Control hindbrain explant showing symmetrical outgrowth. Midline floor plate region is indicated (FP). (B) Hindbrain explant cultured with roof plate explant (RP). (C) Hindbrain explant co-cultured with trigeminal ganglion explant (VG). (D) Lower right portion of hindbrain explant showing labelled motor axons growing towards a trigeminal ganglion explant (VG). Scale bar, 300 μ m (A-C), and 150 μ m (D).



promoting effect of the branchial arch (see Materials and Methods).

To ascertain whether this activity was capable of reorienting axons, branchial arch explants were juxtaposed to the rostral or the caudal end of hindbrain explants. In these cultures, some motor axons deflected from lateral paths and arced towards the arch tissue; there was a large increase in the number of axons extending from the rostral or caudal end of the explant adjacent to the arch (Fig. 5C,E). For hindbrain controls, growth quantitated from the rostral and caudal explant edges was symmetrical, compared with the highly asymmetrical outgrowth along the rostrocaudal axis in the presence of the branchial arch (Fig. 6B).

In order to test further the case for chemoattraction, we cultured hindbrain explants in tandem alongside a branchial arch explant (Fig. 5F). This experimental paradigm has previously been used by Lumsden and Davies (1983) to distinguish between a chemoattractive and a growth-promoting effect of a secreted molecule. The basis of this assay is that a molecule with chemoattractive properties should elicit outgrowth from the near side of the distal explant that is greater than outgrowth from the far side of the proximal explant. Such a pattern of outgrowth was observed for explants of spinal motor neurons displaying chemoattraction in response to limb bud or sclerotome explants (Ebens et al., 1996). Semi-quantitative analysis showed that in control cultures of hindbrain explants in tandem, growth was symmetrical from each explant (Figs 5D, 4I,J; Table 2). In co-cultures of tandem hindbrains with branchial arch, proximal explants displayed enhanced outgrowth relative to distal explants. In addition, proximal explants were chemoattracted by the arch, showing asymmetrical outgrowth that was significantly different from controls. Among distal explants, chemoattraction was also observed, but to a lesser extent and in fewer cases (Figs 5F, 4I,J). When tested statistically, the chemoattraction shown by distal explants was not significantly different from symmetry (Table 1) and some explants exhibited chemorepulsion (Fig. 6C).

This observation may be accounted for by the fact that axons

at the near side of the distal explant are affected by both chemoattraction from the arch, and chemorepulsion by the floor plate of the proximal explant, in some cases this resulting in symmetrical outgrowth or even chemorepulsion. This phenomenon may also increase the apparent chemoattraction in the proximal explant, since outgrowth from the far side of this explant would be expected to be repelled by the floor plate of the distal explant. Chemorepulsion was not observed in cultures of tandem controls, probably because the overall level of outgrowth was lower (Fig. 5D). Therefore, analysis of tandem co-cultures was not as straightforward as with explants

Fig. 4. Quantitation of results of chemoattraction and chemorepulsion in co-culture experiments. Results for co-cultures based on the semi-quantitative 0-5 scale of scoring are shown in each bar chart. Hindbrain explants were taken from axial levels r2/3, r4/5, r6 and r7/8. For each co-culture category, axon outgrowth of hindbrain explants in the presence of various tissues is shown. The x axis is the value obtained for outgrowth from the side facing the co-cultured explant minus outgrowth from the side facing away. Thus 0 represents symmetrical outgrowth, negative values represent chemorepulsion and positive values chemoattraction. Along the y axis, each bar represents the percentage of explants showing a particular value. Numbers of explants tested are shown in brackets above each chart. (A) Hindbrain controls. (B) Hindbrain co-cultures with dorsal neural tube and roof plate. (C) Hindbrain co-cultures with E12 trigeminal ganglia. (D) Hindbrain co-cultures with E13 trigeminal ganglia, and with E13 trigeminal ganglia in the presence of NGF. (E) Hindbrain co-cultures with branchial arch placed laterally and with branchial arch in the presence of anti-murine (mHGF) antibodies. (F) Spinal cord co-cultures with branchial arch and with branchial arch in the presence of anti-mHGF antibodies. (G) Hindbrain co-cultures with control (buffer-loaded) beads. (H) Hindbrain co-cultures with human HGF (hHGF)-loaded beads placed laterally and with hHGF-loaded beads in the presence of anti-hHGF antibodies. (I,J) Hindbrain co-cultures with two explants cultured in tandem as controls, or in same configuration with branchial arch placed laterally. HB1 tandem with arch represents explant proximal to the arch, whereas HB2 tandem represents explant distal to the arch. HB1 and HB2 tandem controls are designated arbitrarily.

of trigeminal ganglia or spinal motor neurons which grow radially in vitro (Lumsden and Davies, 1983; Ebens et al., 1996). In these cultures, axons from the far sides of explant reoriented in response to chemoattraction, by growing across the tissue explant, whereas in our hindbrain explants axon tracing shows that motor axons did not cross the floor plate

(e.g. Fig. 5G,H). We attempted to overcome these problems by removing the floor plate tissue from ventral explants and dissecting each explant into a number of small fragments, which were then co-cultured with the branchial arch. However, in these cultures motor axons still grew out in a highly polarised fashion, to some extent irrespective of the position of

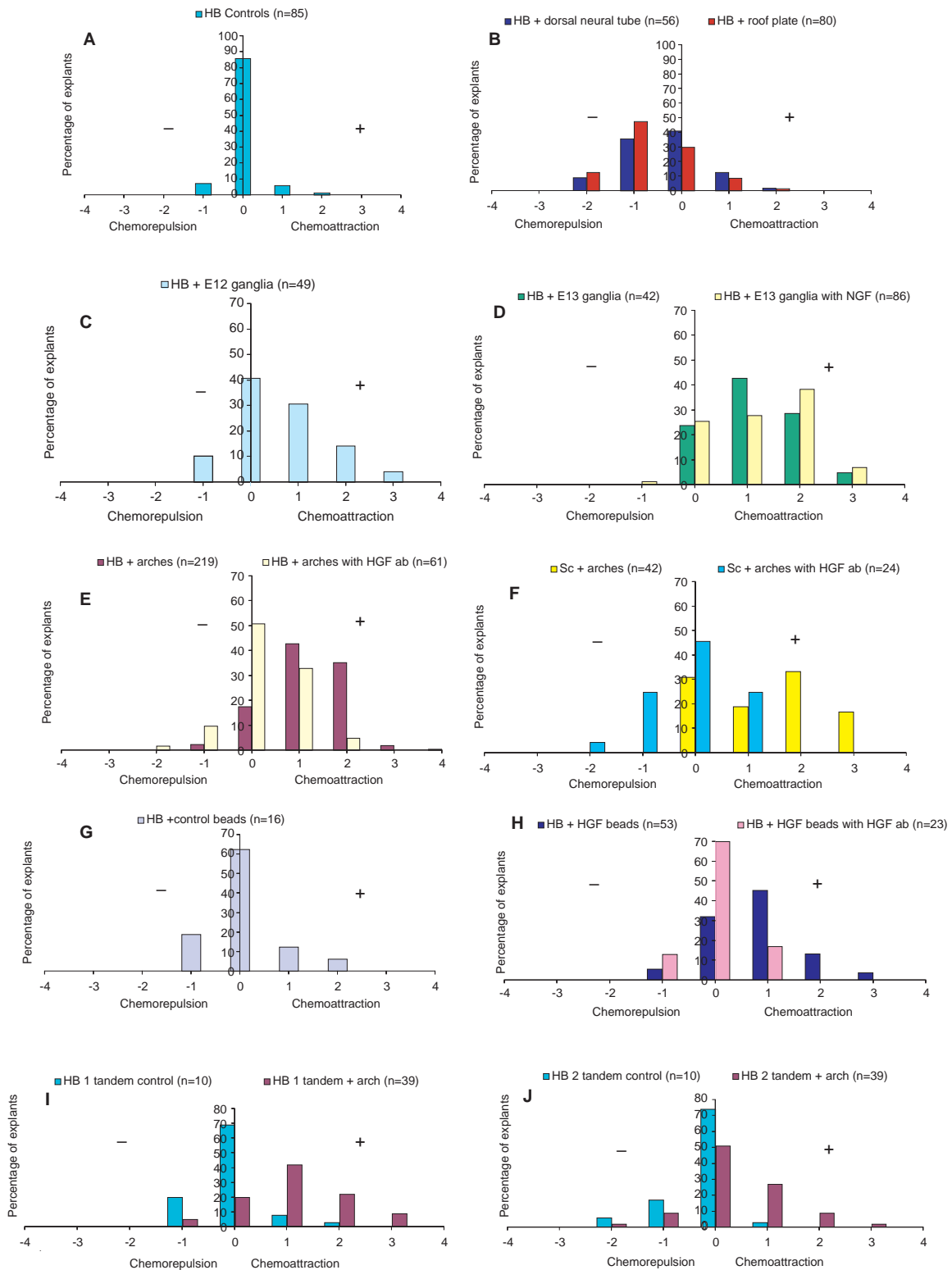


Table 1. Statistical testing of chemoattraction and chemorepulsion in co-cultures with different tissues, using semi-quantitative analysis

Type of co-culture	Is outgrowth asymmetrical? ($P < 0.05$)	Does the pattern of outgrowth change in the presence of anti-HGF antibody? ($P < 0.05$)	Is the pattern of outgrowth in the presence of anti-HGF antibody different from symmetry? ($P < 0.05$)
HB controls	X		
HB + dorsal neural tube	✓		
HB + roof plate	✓		
HB + E12 V ganglion	✓		
HB + E13 V ganglion	✓		
HB + E13 V ganglion+NGF	✓		
HB + branchial arch	✓	✓	✓
HB controls (rostral/caudal)	X		
HB + branchial arch (rostral/caudal)	✓	✓	✓
HB 1 tandem control	X		
HB 2 tandem control	X		
HB 1 tandem + arch	✓		
HB 2 tandem + arch	X		
HB + control beads	X		
HB + HGF beads	✓	✓	X
HB + control beads (rostral/caudal)	X		
HB + HGF beads (rostral/caudal)	✓	✓	X
SC+ branchial arch	✓	✓	X

All co-cultures in lateral orientation unless otherwise stated.

Data was compared statistically using Wilcoxon or Mann-Whitney U-test. For numbers in each category of co-culture see Figs 3 and 4. HB, hindbrain explant; V ganglion, trigeminal ganglion; SC, spinal cord explant. Blank squares are where comparisons were inappropriate or were not made.

Table 2. Statistical testing of chemoattraction in co-cultures, using semi-quantitative and quantitative analysis

Type of co-culture	Semi-quantitative scoring Is outgrowth significantly different from symmetry? ($P < 0.05$)	Quantitative scoring (pixel counting) Is outgrowth significantly different from symmetry? ($P < 0.05$)
HB controls (lateral)	X	X
HB+arch (lateral)	✓	✓
HB controls (rostral/caudal)	X	X
HB+arch (rostral/caudal)	✓	✓
HB+control beads (lateral)	X	X
HB+HGF beads (lateral)	✓	✓
HB+control beads (rostral/caudal)	X	X
HB+HGF beads (rostral/caudal)	✓	✓

Data were compared statistically using Wilcoxon or Mann-Whitney U-test. For numbers in each category of co-culture see Figs 3 and 4.

the branchial arch explant, as if responding to directional cues within the neuroepithelium (data not shown). We therefore conclude that arch-derived chemoattractant molecules are incapable of predominating over cues intrinsic to the neuroepithelium, and can only reorient cranial motor axons within the collagen gel (Fig. 5C,E).

Branchial arch-mediated chemoattraction can be demonstrated using semi-quantitative and quantitative methods

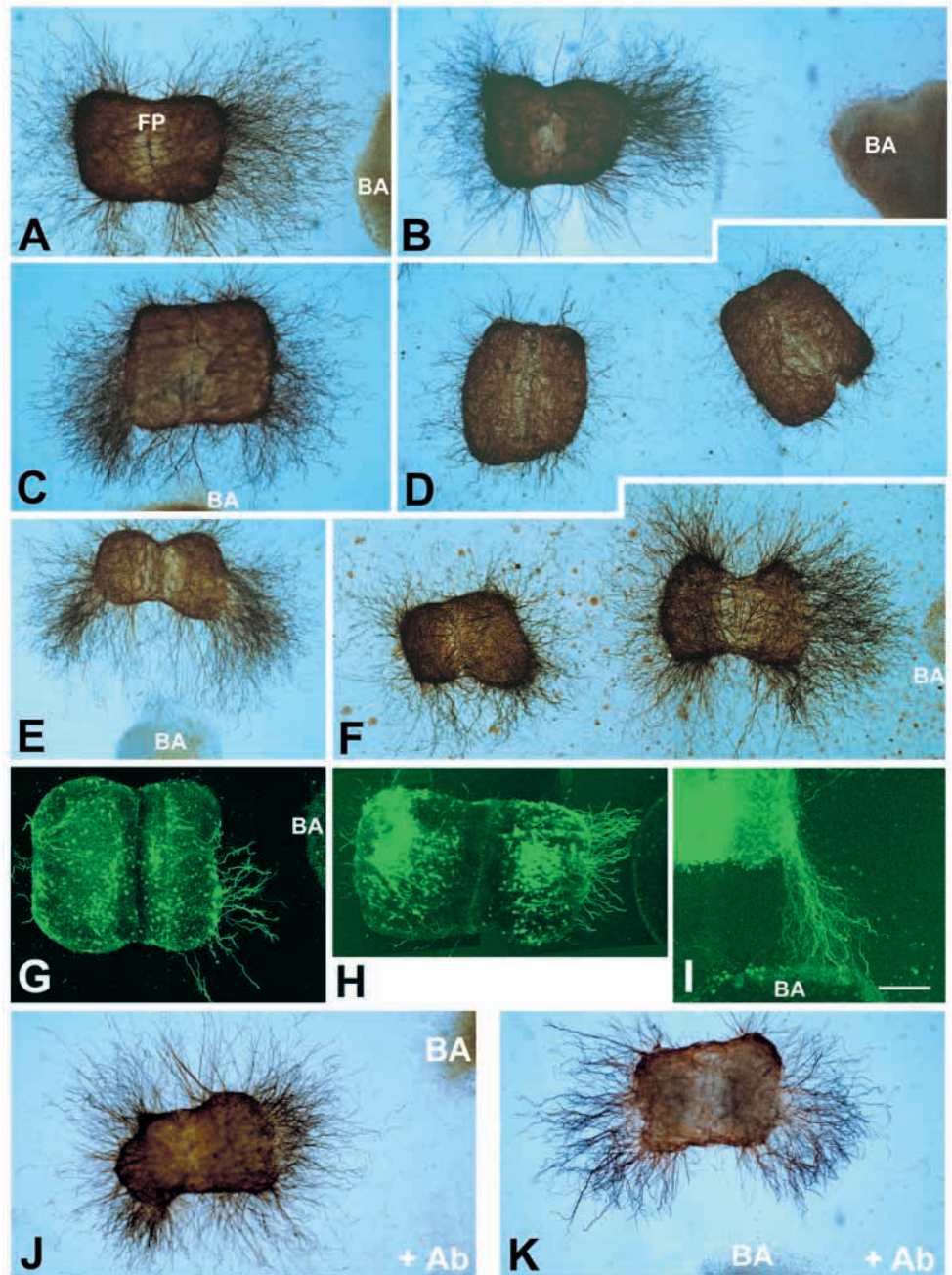
To provide a comparison with our semi-quantitative analysis of cultures, images of immunostained gels were scanned into the computer and axon outgrowth was measured by counting

pixels (see Materials and Methods). Mean numbers of pixels in quadrants facing towards and away from co-cultured tissues were derived (Fig. 6E), and differences between outgrowth towards and away facing quadrants were tested statistically (Table 2). For hindbrain controls, outgrowth was symmetrical when counted from either lateral or rostral/caudal borders. Growth from the lateral or rostral/caudal sides of hindbrains juxtaposed to branchial arches was significantly greater than that from the away-facing sides (Fig. 6E; Table 2).

Several cranial motor axon subpopulations are chemoattracted by the branchial arch

Trigeminal or facial motor neuron explants co-cultured either with their appropriate branchial arch targets (arch 1 or 2 respectively) or with the inappropriate target showed no apparent preference for outgrowth towards the correct target (data not shown). Since only BM axons (trigeminal, facial, glossopharyngeal, vagus and cranial accessory) innervate the branchial arches, this raises the question of whether only these neurons respond to the branchial arch chemoattractant. Responses of dorsally directed axons (BM and VM classes) was confirmed by retrograde labelling from their exit points, which yielded larger numbers of fluorescently labelled axons growing from the explant side facing the arch tissue than from the away-facing side (Fig. 5G,H). The trigeminal nucleus (r2/r3 explants) contains only BM neurons, showing that neurons of this class respond to the arch influence, but the common pathway of BM and VM axons and the lack of any markers that distinguish these neuronal types means that we are unable to confirm unequivocally whether VM axons respond to the arch influence. However, we were able to test the responses to branchial arch explants of SM neurons by retrograde axonal labelling before culture. We found that abducens and hypoglossal neurons in r5

Fig. 5. Responses of cranial motor axons to branchial arch explants. (A-F) Co-cultures immunostained using anti-neurofilament antibodies. (G-I) Co-cultures in which motor axons were retrogradely labelled before co-culture and confocal images obtained after culture. (A,B) Hindbrain explants cultured with branchial arch explant placed laterally. (C,E) Hindbrain explant cultured with branchial arch explant placed rostrally or caudally of the hindbrain explant. Branchial arch explant is below. (D) Tandem control hindbrain explants. (F) Tandem hindbrain explants cultured with branchial arch explant. (G,H) Hindbrain explant in which dorsally projecting motor axons have been retrogradely labelled before culture. (G) Facial motor neurons in an r4/5 explant and (H) glossopharyngeal motor neurons in an r6 explant. (I) Hindbrain explant in which ventrally projecting hypoglossal motor axons have been retrogradely labelled before culture of an r8 explant, positioned in rostral/caudal orientation. (J) Hindbrain explant co-cultured with branchial arch explant placed laterally, in the presence of anti-mHGF antibodies. (K) Hindbrain explant cultured in the presence of branchial arch explant placed rostral/caudal, in the presence of anti-mHGF antibodies. BA, branchial arch; FP, floor plate. Scale bar, 500 μm (A-H), 300 μm (I).



and r7/8 explants respectively displayed chemoattraction to the arch, and reorientation of hypoglossal axons was seen in r7/8 explants placed with rostral/caudal edges facing the arch (Fig. 5I). In addition, trochlear and oculomotor neurons both responded to the branchial arch influence (data not shown). Taken together, these data suggest that outgrowth of a number of groups of cranial motor neurons is affected by a factor produced in the branchial arches, and possibly in other target tissues of the head.

Cranial and spinal motor axons show reciprocal interactions with the branchial arches and the limb buds

We next asked whether this chemoattractant effect was specific

to the branchial arches. Spinal motor neurons have been shown to respond to a chemoattractant secreted by limb bud tissues, raising the possibility that the same chemoattractant could be present in the head and affect cranial motor axons (Ebens et al., 1996). We repeated experiments involving spinal cord explants and limb bud explants and found that whereas spinal cord explants cultured alone showed radial outgrowth (Fig. 7A), in co-cultures with limb bud tissue many explants showed chemoattraction (Fig. 7C). Furthermore, spinal motor axons were chemoattracted by the branchial arches (Figs 7D, 4F). In reciprocal experiments, limb bud tissue was capable of exerting a chemoattractive influence on hindbrain explants (Fig. 7B). These results demonstrate that cranial and spinal motor axons are capable of responding to the chemoattractive influence of

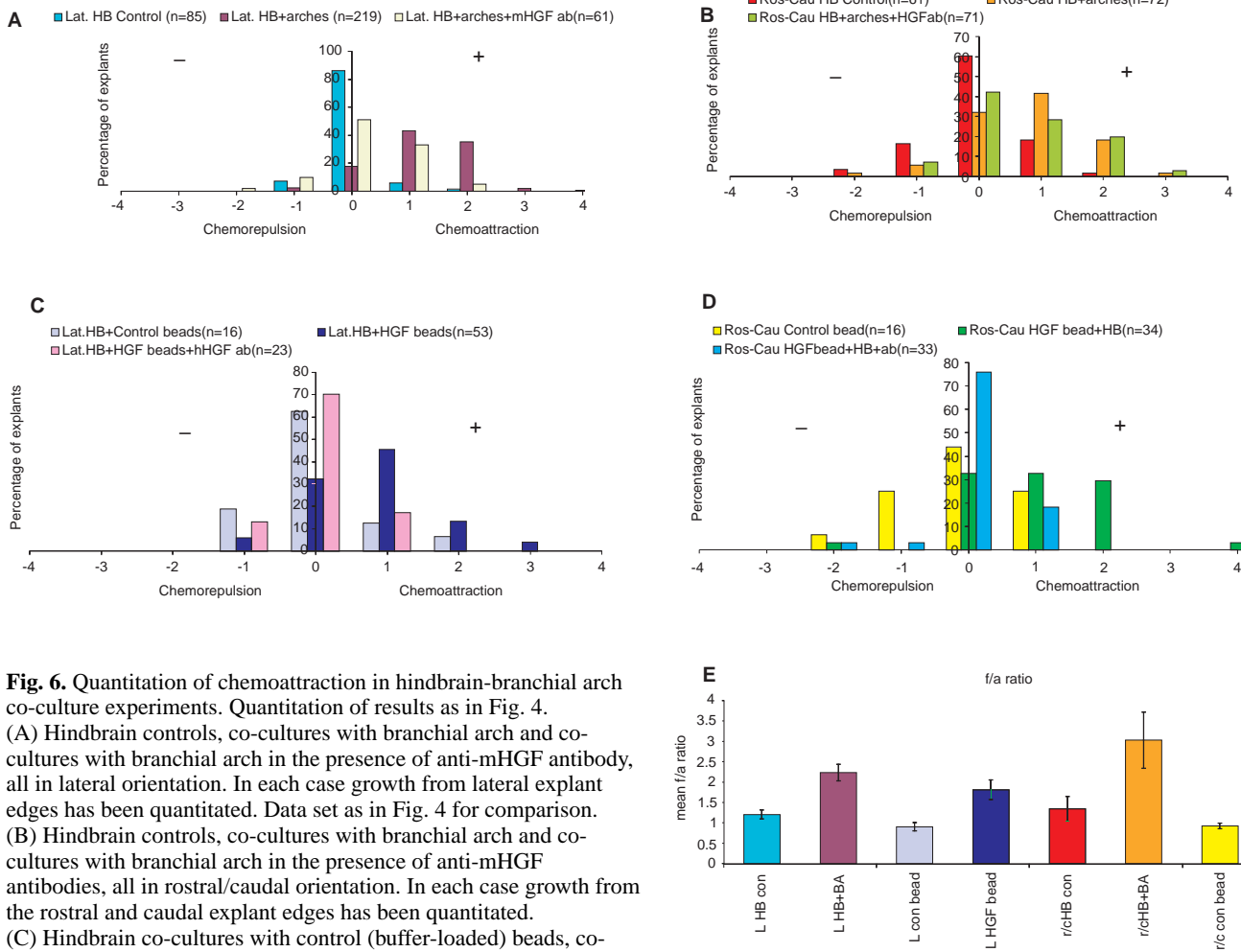


Fig. 6. Quantitation of chemoattraction in hindbrain-branchial arch co-culture experiments. Quantitation of results as in Fig. 4. (A) Hindbrain controls, co-cultures with branchial arch and co-cultures with branchial arch in the presence of anti-mHGF antibody, all in lateral orientation. In each case growth from lateral explant edges has been quantitated. Data set as in Fig. 4 for comparison.

(B) Hindbrain controls, co-cultures with branchial arch and co-cultures with branchial arch in the presence of anti-mHGF antibodies, all in rostral/caudal orientation. In each case growth from the rostral and caudal explant edges has been quantitated.

(C) Hindbrain co-cultures with control (buffer-loaded) beads, co-cultures with hHGF-loaded beads and co-cultures with hHGF-loaded beads in the presence of anti-hHGF antibodies, all in lateral orientation. In each case growth from lateral explant edges has been quantitated.

Data set as in Figure 4 for comparison. (D) Hindbrain co-cultures with control (buffer-loaded) beads, co-cultures with hHGF-loaded beads and co-cultures with HGF-loaded beads in the presence of anti-hHGF antibodies, all in rostral/caudal orientation. In each case growth from rostral and caudal explant edges has been quantitated.

(E) Graph showing quantitative data (computer scoring) from hindbrain-branchial arch co-cultures. X axis shows category of co-culture. Y axis shows axon outgrowth from facing side/away facing side expressed as a mean ratio. L HB con ($n=203$), L HB + BA ($n=18$), L con bead ($n=15$), L HGF bead ($n=21$), r/c HB con ($n=10$), r/c HB + BA ($n=20$), r/c con bead ($n=10$), r/c HGF bead ($n=10$). L, lateral orientation; r/c, rostral/caudal orientation; con, control; HB, hindbrain; BA, branchial arch..

the other's target, and imply that limb bud may contain the same chemoattractant (s) as the branchial arch.

Is Hepatocyte Growth Factor the branchial arch chemoattractant?

The chemoattractant effect of limb bud tissues on spinal motor neurons could be blocked by neutralising antibodies to HGF (Ebens et al., 1996), suggesting that HGF is produced in the periphery. Given that cranial and spinal motor neurons can both respond to limb and arch-secreted factors, it is possible that the arch-secreted factor is also HGF. To test this possibility, human HGF protein was loaded on to heparin-acrylic beads, which were co-cultured lateral to hindbrain explants. Cranial motor axons showed increased outgrowth in the presence of HGF-loaded beads when compared with responses to control beads incubated in buffer (Figs 4G,H, 7E,F). There was a striking reorientation of axons towards HGF-loaded beads when the latter were cultured in rostro-caudal orientation relative to

hindbrain explants (Fig. 7H). This chemoattractant effect was significant, compared with no effect on direction of axon outgrowth by control beads placed in rostrocaudal orientation (Figs 6D, 7H,I). These effects of HGF-loaded beads in both orientations were also significant when compared using quantitative methods (Fig. 6E; Table 2). When an antibody to human HGF was applied to cultures with HGF-loaded beads placed either in lateral or in rostrocaudal orientation, HGF-mediated outgrowth and chemoattraction was completely blocked since axon outgrowth was not significantly different from controls (Figs 4G,H, 6C,D, 7G,J; Table 1).

To test the idea that the branchial arch chemoattractant is HGF, we investigated whether the arch-mediated chemoattraction could be blocked using a neutralising antibody against murine HGF (kind gift from E. Gherardi) which also recognises rat HGF (Ebens et al., 1996). Co-cultures of hindbrain and branchial arch explants with and without antibody were scored blind. The results showed that the

chemoattractive effect of the branchial arch tissue placed lateral to the hindbrain explant was significantly reduced by these anti-HGF antibodies (Figs 4E, 5J). However, the outgrowth of hindbrain explants cultured with branchial arches in the presence of neutralising antibodies to HGF was still significantly different from symmetrical outgrowth, with 37.7% of explants still displaying chemoattraction (Fig. 4E; Table 1). We based the concentration of antibody used on previous studies (20–30 $\mu\text{g/ml}$; Ebens et al., 1996), and found that increasing the concentration of antibody in the cultures to 75 $\mu\text{g/ml}$ failed to achieve a more complete block of chemoattraction (data not shown). Similarly, varying the amount of arch tissue used in the co-cultures did not make an appreciable difference to the degree of antibody block obtained. Closely similar results were obtained when anti-HGF antibodies were applied to cultures of hindbrain explants with branchial arches in rostrocaudal orientation. The dramatic redirecting of axons towards the branchial arch was strongly reduced, but not entirely eliminated in the presence of these antibodies (compare Fig. 6K with 5C and E). As with the experiments in lateral juxtaposition, the distribution of outgrowth along the rostrocaudal axis was significantly reduced, but still differed from symmetry (Fig. 6B; Table 1).

To provide a comparison, we applied anti-HGF antibodies to spinal cord explants co-cultured with branchial arches. In contrast with the incomplete block obtained in hindbrain and branchial arch cultures, the chemoattractant effect of branchial arch tissue on spinal motor axons was completely blocked, i.e. reduced to a level equivalent to symmetry by application of antibodies, implying that this effect is mediated by HGF (Fig. 4F; Table 1; Ebens et al., 1996). The residual chemoattraction from the arch on cranial motor axons in the presence of antibody argues for the existence of a separate factor or factors in the branchial arches which may be specific in its effects on cranial motor neurons.

Expression of *HGF* and *Met* in early embryos

Expression patterns of *HGF* in early rat and chick embryos were examined using in situ hybridisation. In E11–12 rat embryos, we found that *HGF* was expressed in the limb buds as reported previously (Ebens et al., 1996) and in the first branchial arch (Fig. 8A–C). At E12, stripes of expression were observed in branchial arches 1–3 in central regions likely to be occupied by myogenic cells (Fig. 8B). An additional stripe of expression appeared to coincide with the region of the cardiac outflow tract. No expression was observed in the extraocular muscles, possibly owing to the small size of the muscle anlage at this stage. In E4 chick embryos,

expression of *HGF* was observed in regions of the branchial arches corresponding to the muscle masses and in two of the extraocular muscles (Fig. 8D).

Localisation patterns of the HGF receptor, *Met*, were

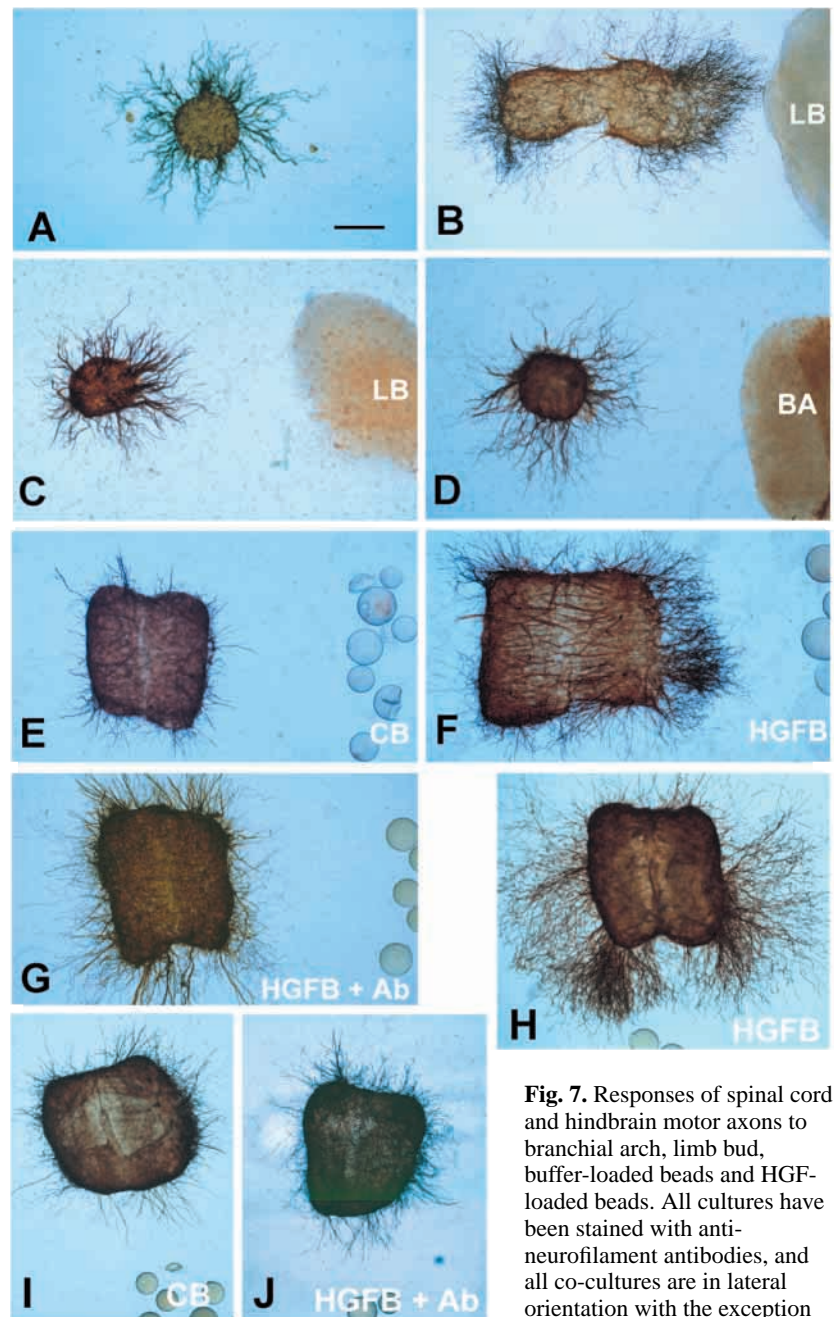


Fig. 7. Responses of spinal cord and hindbrain motor axons to branchial arch, limb bud, buffer-loaded beads and HGF-loaded beads. All cultures have been stained with anti-neurofilament antibodies, and all co-cultures are in lateral orientation with the exception of H, I and J which are in

rostral/caudal orientation. (A) Spinal cord explant control. (B) Hindbrain explant co-cultured with limb bud explant (LB). (C) Spinal cord explant co-cultured with limb bud explant (LB). (D) Spinal cord explant co-cultured with branchial arch explant (BA). (E) Hindbrain explant co-cultured with control, buffer-loaded beads (CB). (F) Hindbrain explant co-cultured with hHGF-loaded beads (HGFB). (G) Hindbrain explant co-cultured with hHGF-loaded beads in the presence of anti-hHGF antibodies (HGFB + Ab). (H) Hindbrain explant co-cultured with hHGF-loaded beads (HGFB; rostral-caudal orientation). (I) Hindbrain explant co-cultured with control, buffer-loaded beads (CB; rostral-caudal orientation). (J) Hindbrain explant co-cultured with hHGF-loaded beads in their presence of anti-hHGF antibodies (HGFB + Ab; rostral-caudal orientation). Scale bar, 500 μm .

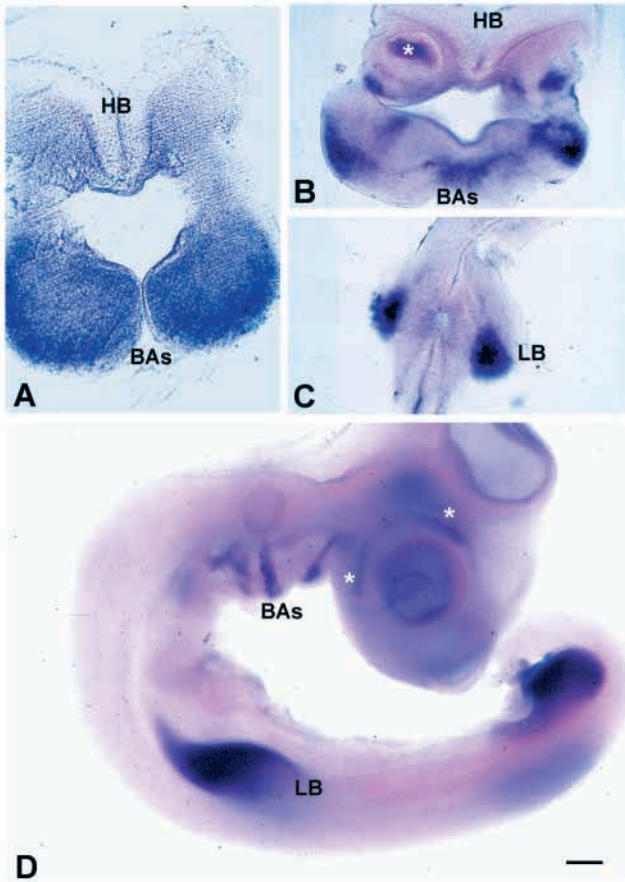


Fig. 8. Expression patterns of HGF in rat and chick embryos. (A) Transverse section through the region of the hindbrain (HB) and the first branchial arches (BAs) in an E11 rat embryo in situ hybridised for *HGF*. Signal is widespread throughout the arches. (B) Transverse section through the region of the hindbrain (HB) and the second branchial arches (BAs) in an E12 rat embryo in situ hybridised for *HGF*. Signal is restricted to specific regions within the branchial arches. (C) Transverse section through the region of the forelimb bud (LB) in an E12 rat embryo. (D) Whole-mount *HGF* in situ hybridisation of stage 21 chick embryo showing stripes of expression in the branchial arches (BAs), in the limb buds (LB) and in two regions close to the eye that may correspond to two of the extra-ocular muscles (white asterisks). Scale bar, 150 μ m (A), 350 μ m (B,C), 500 μ m (D).

compared with those of *Islet 1* in the brainstem of mouse embryos, using single and double in situ hybridisation (Fig. 9). Since *Islet 1* is expressed by all cranial motor neurons at early stages in development (Varela-Echavarría et al., 1996) this allowed us to assess whether all motor neurons or a subpopulation expressed the receptor. At E10 no *Met* expression was observed in the brainstem (data not shown), but from E11-13 domains of *Met* expression could be recognised within the regions corresponding to some of the cranial motor nuclei, with the exception of the oculomotor nucleus. At E12 for example *Islet 1* is clearly expressed in the region of the oculomotor nucleus (labelled III; Fig. 9E), but *Met* is not detectable in this region (Fig. 9B). There was a clear positional registration between the cells expressing *Met* and those expressing *Islet 1*, for example in the region of the trigeminal

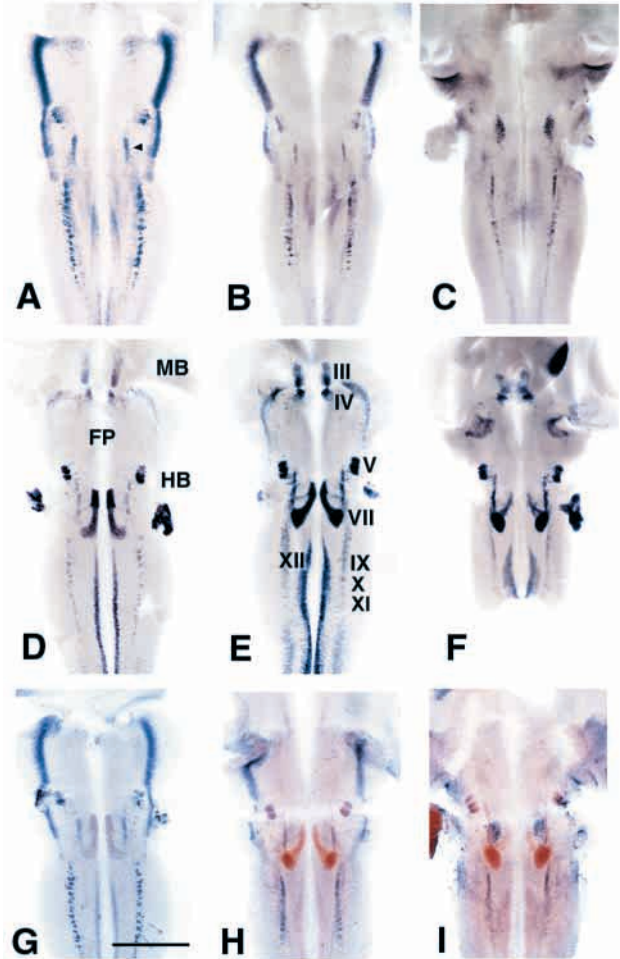


Fig. 9. Expression patterns of *Met* and *Islet 1* in mouse embryos from E10-E12. All panels show dorsal views of the midbrain and hindbrain region of mouse embryos in situ hybridised for *Met* (A-C), *Islet 1* (D-F) or double-labelled with *Met* (blue) and *Islet 1* (red) probes (G-I). Embryonic stages are E11 (A,D,G), E12 (B,E,H), and E13 (C,F,I). *Islet 1* labels differentiating motor neurons. The various motor nuclei are labelled in E. These are III, oculomotor; IV, trochlear; V, trigeminal; VII, facial and superior salivatory; IX, glossopharyngeal; X, vagus; XI, cranial accessory and XII, hypoglossal. The VIth nucleus (abducens) is not apparent as it coincides with the facial nucleus in rhombomere 5. *Met* signal corresponds to a subset of the regions occupied by developing motor neurons as shown by the double in situ hybridisations (G-H). Arrowhead in A shows superior salivatory nucleus in r5 containing VM VIIth nerve neurons. Scale bar, 1 mm.

nucleus (V; Fig. 9A,B,E,H). In other cases, *Met* expression within a motor nucleus appeared to be restricted to a subset of neurons. For example, *Met* expression was absent from the facial motor nucleus (labelled VII in Fig. 9E), which forms a crescent extending from r4 to r6, corresponding to a stream of neurons migrating in a posterior direction (Studer et al., 1996). However, lateral to the facial motor nucleus, *Met* is expressed in a group of cells which represent the superior salivatory nucleus in r5 (arrow in Fig. 9A). In addition, *Islet 1*-positive trochlear motor neurons (marked IV in Fig. 9E) could correspond to the region of *Met* expression just caudal to the midbrain-hindbrain boundary (Fig. 9B) but these cells

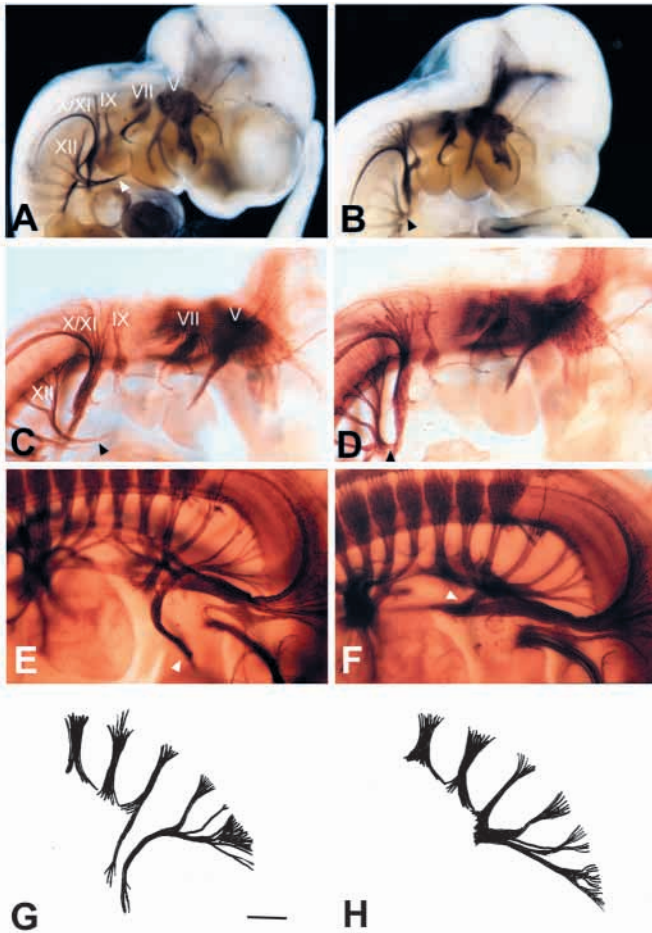


Fig. 10. Neurofilament staining of mouse embryos with targeted disruptions of *HGF* or *Met*. All views of embryos are lateral with rostral to the right. (A-D) E10.5 embryos, (E-H) E11.5 embryos. Arrowheads in A-F show position of the hypoglossal nerve. (A) *HGF*^{+/+} control embryo showing morphology of the cranial nerves. V, trigeminal; VII, facial; IX, glossopharyngeal; X/XI, vagus; cranial accessory; XII, hypoglossal. (B) *HGF* mutant embryo. All cranial nerves are normal with the exception of the hypoglossal nerve which is truncated, and has failed to grow rostrally through the branchial arches. (C) *Met*^{+/+} control embryo. Cranial nerves labelled as in (A). (D) *Met*^{DD} mutant embryo. All cranial nerves are normal with the exception of the hypoglossal, which has a morphology closely similar to that in the *HGF* mutant. (E) Higher magnification of *Met*^{+/+} control embryo. (F) Higher magnification of *Met*^{-/-} embryo. (G) Camera lucida drawing of normal hypoglossal pathway in *Met*^{+/+} embryo. (H) Camera lucida drawing of truncated hypoglossal nerve in *Met*^{DD} embryo. Scale bar, 500 μ m (A,B); 330 μ m in (C,D) and 250 μ m (E,F).

appeared to form a more diffuse cluster than those defined by *Isl1* staining. The more caudal groups of motor neurons, the glossopharyngeal, vagus and cranial accessory (IX, X and XI) and hypoglossal nuclei (XII) also express *Met* (Fig. 9B,E,H). The pattern of *Met* expression observed at E13 (Fig. 9C) was closely similar to that at E12. Staining was also observed in dorsal regions in rhombomere 1, which may correspond to the developing cerebellum (Fig. 9A,B).

BM and VM neurons undergo a medial to lateral migration within the brainstem during their maturation (Simon et al., 1994). The localisation of *Met* in lateral regions therefore

suggests that this receptor is expressed in older motor neurons that have already extended axons into the periphery. If this cohort of neurons represents only a subpopulation within each nucleus, then it may be the earliest cohort to differentiate, representing the pioneer neurons that first extend axons peripherally. Axon tracing coupled with expression studies would be needed to clarify this as well as to confirm expression by particular neuronal subpopulations. This far it appears that at least a subpopulation of each motor nucleus, with the exception of the oculomotor and the facial motor nucleus, express *Met*.

Cranial nerve morphology in mice with targeted disruptions of *HGF* and *Met*

In order to further investigate a possible role for *HGF* signalling in cranial motor axon pathfinding we examined mice with targeted disruptions of the genes encoding *HGF* (Schmidt et al., 1995) or *Met* (the *Met*^{DD} mutant; Maina et al., 1996). Anti-neurofilament staining of E10.5 embryos revealed the axonal pathways in the cranial region of wild-type embryos (Fig. 10A,C). In *HGF*^{-/-} embryos these nerve pathways looked superficially similar, except for the hypoglossal nerve, which was truncated (arrow in Fig. 10B). This reflects a failure of this nerve to grow along its normal course rostrally through the branchial arches (Fig. 10C,E,G). A closely similar phenotype was observed in *Met*^{DD} embryos (Fig. 10D,F,H). Since *HGF*-*Met* signalling is required for correct migration of a subset of tongue myoblasts (Bladt et al., 1995), this defect might be interpretable in terms of a loss of the synaptic targets of hypoglossal axons. However, in the *Met*^{Grb2/Grb2} mutant these muscles develop correctly, and yet a defect in the hypoglossal nerve is still observed (F. M. and R. K., unpublished data). In addition, *HGF* expression may not be restricted to myogenic precursors, since it is present along the pathway of the hypoglossal nerve in *Met* mutants which lack these migrating cells (Dietrich et al., 1999). This suggests that aberrant hypoglossal nerve outgrowth is due to a direct effect of loss of *HGF*-*Met* signalling on axon guidance. Observation of *HGF*^{-/-} embryos at later stages of development, however, indicate that the delay in hypoglossal outgrowth is compensated at later stages of development, perhaps by other guidance mechanisms. Other cranial nerve pathways appeared normal in the mutant embryos, suggesting that additional guidance mechanisms operate, perhaps including branchial arch chemoattractants that are distinct from *HGF*.

DISCUSSION

In this study we have explored the possible influences of diffusible guidance molecules produced by pathway tissues on cranial motor axon navigation. Our major conclusion is that the branchial arches exert a growth-promoting and chemoattractant influence on motor axons as they extend towards their peripheral targets. Since anti-*HGF* antibodies block this interaction in vitro, this effect is at least partially mediated by *HGF*. *HGF* is expressed in regions corresponding to developing muscles, including those of the branchial arches, and is capable of causing increased outgrowth and orientation of motor axons of all classes, suggesting that it is a general cue for axon outgrowth in the head, rather than a signal that governs specific

wiring of cranial motor axons to their targets. The HGF receptor *Met* is present in only a subset of cranial motor neurons, and disruption of *HGF* or *Met* gene function produces only minor defects in cranial motor axon pathfinding. Thus, additional arch-derived chemoattractants or other guidance molecules are implicated in pathfinding to the branchial arches.

The neuroepithelium of the dorsal neural tube, which contains the exit point, fails to chemoattract motor axons, and so cannot account for the navigation of axons towards this region. Both the dorsal neural tube and the roof plate are inhibitory and/or chemorepellent, and may provide a stop signal that limits the dorsal growth of cranial motor axons. The growth promoting and/or chemoattractant effect of the cranial sensory ganglia on cranial motor axons may depend upon mesenchymal cells isolated together with the ganglia.

HGF is a guidance cue for cranial motor axons

We have shown that cranial motor axons exhibit increased growth and chemoattraction in response to branchial arch tissues, and that anti-HGF antibodies partially block arch-mediated chemoattraction. Coupled with observations of hypoglossal nerve defects in *HGF*^{-/-} and *Met*^{D/D} mutant embryos, this implies that HGF is an important factor produced by the arches which participates in motor axon guidance. In support of this idea were our findings that HGF presented on beads can chemoattract cranial motor axons. These data are consistent with previous studies showing that chemoattraction of spinal motor axons by the limb bud depends on HGF (Ebens et al., 1996), and that mouse embryos mutant for *HGF* or *Met* display defects in motor nerve branching within the limbs, as well as in sensory innervation of the limbs and thorax (Ebens et al., 1996; Maina et al., 1997). Our findings extend the repertoire of known roles for HGF, which in addition to influencing the growth of motor neurons, promotes the outgrowth and survival of DRG sensory neurons (Maina et al., 1997) and the outgrowth of sympathetic neurons (Maina et al., 1998).

The precise localisation of HGF in the tissues of the head requires further investigation, including double labelling studies using muscle markers. We found *HGF* to be expressed by branchial arch tissues in both rat and chick embryos (see also Théry et al., 1995), and in the latter, this region overlapped with the muscle plate containing immigrant myogenic precursors. In the limb, HGF is not expressed by muscle cells, but is confined to the lateral plate mesoderm (Ebens et al., 1996). Recent studies also showed the expression of HGF along the pathway of tongue muscle precursors in the absence of these cells, pointing to additional mesenchymal cell populations as a source of HGF (Dietrich et al., 1999). Certainly, a wider axon guidance role of HGF than is reflected simply by its production by the branchial arches is also implied by the expression of this factor by the extra-ocular muscles (Fig. 8D). Possibly HGF is involved in pathfinding of many motor axon populations, but close spatiotemporal regulation prevents axons growing aberrantly. Consistent with this were findings that branchial arches chemoattracted both BM axons (their normal innervation) and SM axons. Diffusion of HGF might be limited by tissues such as the presumptive cartilage, which acts as a barrier to motor axon outgrowth (Tosney, 1991), or by binding to components of the extracellular matrix.

Insights into the role of HGF will also come from studying,

in more detail, the regulation of *Met* expression during motor neuron development, since we observed restricted *Met* expression by subpopulations of cranial motor neurons at a later phase of their pathfinding into the periphery. In the spinal cord *Met* is also expressed in a restricted pattern, being present at high levels within brachial level motor neurons destined to innervate the limbs, and at much lower levels in spinal motor neurons at other axial levels (Ebens et al., 1996; Yamamoto et al., 1997).

Is there an additional chemoattractant activity in the head?

A number of hindbrain explants cultured with branchial arches and anti-HGF antibodies exhibited a significant degree of chemoattraction. We believe that this effect is unlikely to be due to degradation of the antibody in the culture system, since in tests we found that the degree of chemoattraction manifest was equivalent at 24 hours and at 36-40 hours after the beginning of culture, and increasing the antibody concentration did not inhibit the chemoattraction more completely. The observation that chemoattraction of cranial motor axons by HGF-loaded beads was completely blocked by antibodies also shows that technical constraints are unlikely to account for the absence of block observed in branchial arch co-cultures. These data therefore lead to the conclusion that an additional chemoattractive factor may be generated by the branchial arches.

Two other lines of evidence support the idea of additional chemoattractants. First, only a subset of cranial motor neurons expressed the HGF receptor *Met*, despite the fact that all motor axon subpopulations tested were chemoattracted by the arch. It seems unlikely that HGF acts on cranial motor axons by binding to a receptor other than *Met*; there is a close correlation between the phenotypes of animals mutant for *Met* and for *HGF* (Bladt et al., 1995; Schmidt et al., 1995; Uehara et al., 1995). Secondly, mice carrying targeted disruptions of *HGF* and *Met* showed modest defects in the pathfinding of the hypoglossal nerve, indicating a role for HGF-*Met* signalling in hypoglossal nerve outgrowth. However, the integrity of other cranial nerve pathways was preserved, pointing to the existence of additional axon guidance factors. We will aim to test this possibility by co-culturing cranial motor axons with branchial arches derived from *HGF*^{-/-} mice, and investigating whether chemoattraction is still present.

What is the role of the exit point, roof plate and cranial sensory ganglia?

The roles of tissues other than the branchial arches in cranial motor axon guidance deserve to be investigated further. The dorsal neural tube, which may contain elements of the exit point, proved to be inhibitory and/or chemorepellent, despite previous evidence of its chemoattractive role (Guthrie and Lumsden, 1992). This may not be surprising, given that exit point-forming cells might be too few in number to exert chemoattraction in collagen gels. Exit point signals might arise from a late-emigrating population of hindbrain neural crest cells, which in the chick form the dorsal exit points (Niederländer and Lumsden, 1996). These cells, or adjacent mesenchymal cells, might be lost during preparation of dorsal neural tube explants. Studies on the dorsal root entry zone of the spinal nerves in the chick have shown that similar clusters

of 'boundary cap' cells are likely to be involved in the guidance of incoming dorsal root afferents and the establishment of a non-permissive region for later axon ingrowth (Golding and Cohen, 1997). If they do not act exclusively by chemoattraction, boundary cap cells might guide outgrowing motor axons by contact-mediated interactions. In the case of chemoattraction by the cranial ganglia, we believe that this is not a phenomenon distinct from branchial arch chemoattraction, but instead is most likely to be due to contaminating mesenchyme cells which are difficult to remove and also proliferate extensively in collagen gel cultures. Among these cells may be myogenic precursors or other mesenchymal cells which express HGF. Possible candidates to mediate dorsal neural tube/roof-plate dependent chemorepulsion may be Semaphorin 3D (previously collapsin 2), based on its localisation on either side of the roof plate in the spinal cord (Luo et al., 1995), or BMPs, based on their expression in the roof plate and ability to repel commissural axons (Liem et al., 1995; Augsburger et al., 1999).

Sequential steps in cranial motor axon guidance

Early cranial motor axon pathway choices reflect the BM/VM or SM phenotypes of neurons that differentiate in response to graded activity of Sonic Hedgehog (SHH) protein (reviewed by Tanabe and Jessell, 1996). An early step in SHH induction is the expression of the transcription factor *MNR2*, which is required for the differentiation of SM but not BM/VM neurons (Tanabe et al., 1998). In addition, *Pax6* is expressed in a dorsoventral gradient in response to SHH signalling, and whilst BM/VM neurons differentiate within a ventral, *Pax6*-negative domain of the neuroepithelium, SM neurons differentiate within a more dorsal domain of low *Pax6* expression (Ericson et al., 1997). In mice and rats lacking *Pax6*, ventrally projecting hindbrain SM neurons fail to differentiate and may assume the fates of BM/VM neurons (Ericson et al., 1997; Osumi et al., 1997). However, *Pax6* appears to act indirectly, by controlling the expression of *Nkx2.2*, since in mice mutant for this gene, spinal ventral interneurons assume the fates of more dorsal motor neurons (Briscoe et al., 1999). In the hindbrain, BM/VM neurons normally derive from the *Nkx2.2*-positive domain, but were unaffected in the mutant, and the authors speculate that another transcription factor (perhaps *Nkx2.9*) assumes the function of assigning motor neuron fates in this region (Briscoe et al., 1999).

Downstream of these early events, dorsal or ventral motor axon pathway choices appear to be under the control of LIM homeodomain transcription factors, which are expressed in a combinatorial manner among motor neuron subpopulations in the chick embryo (Tsuchida et al., 1994; Varela-Echavarría et al., 1996). In mouse embryos deficient for two of these factors, *Lhx3* and *Lhx4*, ventrally projecting motor neurons change their identity and form dorsal axon projections, whilst misexpression of *Lhx3* in dorsally projecting neurons causes them to reorient their projections ventrally (Sharma et al., 1998). Formation of an exit point therefore appears cell autonomous in the case of ventrally projecting neurons, even if additional cells are recruited to the exit site once formed.

An early hallmark of differentiation for ventrally or dorsally projecting neurons is presumably expression of receptors for chemorepellents expressed at the midline, since motor axons

are repelled by the floor plate (Guthrie and Pini, 1995). Molecules involved in midline repulsion are likely to be Netrin 1 Semaphorin 3A and Slit, (Colamarino and Tessier-Lavigne, 1995; Varela-Echavarría et al., 1997; Brose et al., 1999). Spinal motor neurons express the Slit receptors, Robo 1 and 2 (Brose et al., 1999), but so far there has not been a detailed analysis of the localisation of Robo or of receptors for Netrins and Semaphorins among cranial motor neurons. Since dorsally projecting cranial motor neurons respond to both Netrin 1 and Semaphorin 3A, whereas ventrally projecting cranial motor neurons respond only to the latter molecule (Varela-Echavarría et al., 1997), the expression of receptors for the repulsive effects of Netrin 1 might be more restricted.

For somatic motor neurons of the abducens and hypoglossal nuclei, other cues are required to account for the longitudinal pathways taken. Possibly, HGF is produced by the target muscles of these neurons, the lateral rectus and the tongue muscles respectively. In the case of abducens guidance cues include early contact with the muscle anlage of lateral rectus and coordinate growth/migration of nerve and muscle to their destination adjacent to the eye (Wahl et al., 1994). BM and VM neurons may respond to as yet unidentified polarity cues in the neuroepithelium which guides their course dorsally, and rostrally in the case of axons originating in odd-numbered rhombomeres. Their dorsal trajectory is limited by repulsion by the roof plate and dorsal neural tube. Dorsally projecting axons grow out via the exit points, which already form pathways for incoming sensory axons. Chemoattraction from some component of the exit point and/or contact guidance by sensory neurons is likely to be required for their egress from the neural tube. Once in the periphery, BM axons grow towards the muscle plates of the branchial arches under the influence of HGF and other factors.

Although HGF is one important guidance cue for cranial motor axons, other axon guidance cues are required in this scheme to account for the selectivity and shaping of projections. Notably, Semaphorin 3A appears to be involved in channelling motor axons into the cores of the branchial arches, since in mice mutant for *Semaphorin 3A* or its receptor *Neuropilin 1*, widespread defasciculation of nerves into inappropriate arch regions is observed (Taniguchi et al., 1997; Kitsukawa et al., 1997). Furthermore, little is known of the mechanisms that segregate nerve branches to individual muscles later in development. Understanding how HGF and other guidance cues act *in vivo* will involve a detailed consideration of how these molecules are organised spatiotemporally and interact with each other, in relation to the pathways of different cranial motor nerves.

We thank C. Henderson for valuable discussions about the manuscript and for sharing data with us. We also thank E. Audero, H. Funakoshi, T. Jessell, T. Nakamura, C. Ponzetto and C. Stern for providing *HGF* and *Met* probes, and E. Gherardi for the anti-HGF antibody. This work was supported by a grant from the Wellcome Trust.

REFERENCES

- Augsburger, A., Schuchardt, A., Hoskins, S., Dodd, J. and Butler, S. (1999). BMPs as mediators of roof plate repulsion of commissural neurons. *Neuron* **24**, 127-141.
- Bagnard, D., Lohrum, M., Uziel, D., Püschel, A. and Bolz, J. (1998).

- Semaphorins act as attractive and repulsive guidance during the development of cortical projections. *Development* **125**, 5043-5053.
- Bladt, F., Riethmacher, D., Isenmann, S., Aguzzi, A., and Birchmeier, C.** (1995). Essential role for the c-met receptor in the migration of myogenic precursor cells into the limb bud. *Nature* **376**, 768-771.
- Briscoe, J., Sussel, L., Serup, P., Hartigan O'Connor, Jessell, T. M., Rubenstein, J. L. R. and Ericson, J.** (1999). Homeobox gene *Nkx2.2* and specification of neuronal identity by graded Sonic hedgehog signalling. *Nature* **398**, 622-627.
- Brose, K., Bland, K. S., Wang, K. H., Arnott, D., Henzel, W., Goodman, C. S., Tessier-Lavigne, M. and Kidd, T.** (1999). Slit proteins bind Robo receptors and have an evolutionarily conserved role in repulsive axon guidance. *Cell* **96**, 795-806.
- Colamarino, S. A. and Tessier-Lavigne, M.** (1995). The axonal chemoattractant netrin-1 is also a chemorepellent for trochlear motor neurons. *Cell* **81**, 621-629.
- Dietrich, S., Abou-Rebyeh, F., Brohmann, H., Bladt, F., Sonnenberg-Riethmacher, E., Yamaai, T., Lumsden, A., Brand-Saberi, B. and Birchmeier, C.** (1999). The role of SF/HGF and c-Met in the development of skeletal muscle. *Development* **126**, 1621-1629.
- Dodd, J., Morton, S. B., Karagogeos, D., Yamamoto, M. and Jessell, T. M.** (1988). Spatial regulation of axonal glycoprotein expression on subsets of embryonic spinal neurons. *Neuron* **1**, 105-116.
- Ebens, A., Brose, K., Leonardo, E. D., Gartz Hanson Jr., M., Bladt, F., Birchmeier, C., Barns, B. A. and Tessier-Lavigne, M.** (1996). Hepatocyte Growth Factor/Scatter Factor is an axonal chemoattractant and neurotrophic factor for spinal motor neurons. *Neuron* **17**, 1157-1172.
- Ericson, J., Rashbass, P., Schedl, A., Brenner-Morton, S., Kawakami, A., van Heyningen, V., Jessell, T. M. and Briscoe, J.** (1997). *Pax6* controls progenitor cell identity and neuronal fate in response to graded Shh signalling. *Cell* **90**, 169-180.
- Gilland, E. and Baker, R.** (1993). Conservation of neuroepithelial and mesodermal segments in the embryonic vertebrate head. *Acta Anat.* **148**, 110-123.
- Golding, J. P. and Cohen, J.** (1997). Border controls at the mammalian spinal cord: late-surviving neural crest boundary cap cells at dorsal root entry sites may regulate sensory afferent ingrowth and entry zone morphogenesis. *Mol. Cell Neurosci.* **9**, 381-396.
- Guthrie, S. and Lumsden, A.** (1992). Motor neuron pathfinding following rhombomere reversals in the chick embryo hindbrain. *Development* **114**, 663-673.
- Guthrie, S. and Lumsden, A.** (1994). Collagen gel coculture of neural tissue. *Neuroprotocols* **4**, 116-120.
- Guthrie, S. and Pini, A.** (1995). Chemorepulsion of developing motor axons by the floor plate. *Neuron* **14**, 117-1130.
- Kennedy, T. E., Serafini, T., de la Torre, J. R. and Tessier-Lavigne, M.** (1994). Netrins are diffusible chemotropic factors for commissural axons in the embryonic spinal cord. *Cell* **83**, 161-169.
- Kitsukawa, T., Shimizu, M., Sanbo, M., Hirata, T., Taniguchi, M., Bekku, Y., Yagi, T. and Fujisawa, H.** (1997). Neuropilin-semaphorin D-mediated chemorepulsive signals play a crucial role in peripheral nerve projection in mice. *Neuron* **19**, 995-1005.
- Liem, K. F. Jr., Tremml, G., Roelink, H. and Jessell, T. M.** (1995). Dorsal differentiation of floor plate cells induced by BMP-mediated signals from epidermal ectoderm. *Cell* **82**, 969-979.
- Lumsden, A. G. and Davies, A. M.** (1983). Earliest sensory nerve fibres are guided to peripheral targets by attractants other than nerve growth factor. *Nature* **306**, 786-788.
- Lumsden, A. and Keynes, R.** (1989). Segmental patterns of neuronal development in the chick hindbrain. *Nature* **337**, 424-428.
- Luo, Y., Raible, D. and Raper, J. A.** (1995). A family of molecules related to collapsin in the embryonic chick nervous system. *Neuron* **14**, 1131-1140.
- Maina, F., Casagrande, F., Audero, E., Simeone, A., Comoglio, P., Klein, R. and Ponzetto, C.** (1996). Uncoupling of Grb2 from the Met receptor in vivo reveals complex roles in muscle development. *Cell* **87**, 531-542.
- Maina, F. and Klein, R.** (1999). Hepatocyte growth factor, a versatile signal for developing neurons. *Nature Neurosci.* **2**, 213-217.
- Maina, F., Hilton, M. C., Andres, R., Wyatt, S., Klein, R. and Davies, A. M.** (1998). Multiple roles for hepatocyte growth factor in sympathetic neuron development. *Neuron* **20**, 835-846.
- Maina, F., Hilton, M. C., Ponzetto, C., Davies, A. M., and Klein, R.** (1997). Met receptor signalling is required for sensory nerve development and HGF promotes axonal growth and survival of sensory neurons. *Genes Dev.* **11**, 3341-3350.
- Nakamura, T., Nishizawa, T., Hagiya, M., Seki, T., Shimonishi, M., Sugimura, A., Tashiro, K. and Shimizu, S.** (1989). Molecular cloning and expression of human hepatocyte growth factor. *Nature* **342**, 440-443.
- Niederländer, C. and Lumsden, A.** (1996). Late emigrating neural crest cells migrate specifically to the exit points of cranial branchiomotor nerves. *Development* **122**, 2367-2374.
- Noden, D. M.** (1988). Interactions and fates of avian craniofacial mesenchyme. *Development* **103 Suppl.**, 121-140.
- O'Leary, D. D. M. and Wilkinson, D. G.** (1999). Eph receptors and ephrins in neural development. *Curr. Opin. Neurobiol.* **9**, 65-73.
- Osumi, N., Hirota, A., Ohuchi, H., Nakafuku, M., Limura, T., Kuratani, S., Fujiwara, M., Noji, S. and Eto, K.** (1997). Pax-6 is involved in specification of the hindbrain motor neuron subtype. *Development* **124**, 2691-2972.
- Püschel, A. W., Adams, R. H. and Betz, H.** (1995). Murine semaphorin D is a member of a diverse gene family and creates domains inhibitory for axonal extension. *Neuron* **14**, 941-948.
- Schmidt, C., Bladt, F., Goedecke, S., Brinkmann, V., Zschiesche, W., Sharpe, M., Gherardi, E. and Birchmeier, C.** (1995). Scatter factor/hepatocyte growth factor is essential for liver development. *Nature* **373**, 699-702.
- Sharma, K., Sheng H. Z., Lettieri, K., Li, H., Karavanov, A., Potter, S., Westphal, H. and Pfaff, S. L.** (1998). LIM homeodomain factors *Lhx3* and *Lhx4* assign subtype identities for motor neurons. *Cell* **95**, 817-828.
- Simon, H., Guthrie, S. and Lumsden, A.** (1994). Regulation of SC1/DM-GRASP during the migration of motor neurons in the chick embryo brainstem. *J. Neurobiol.* **25** 1129-1143.
- Stoker, M., Gherardi, E., Perryman, M. and Gray, J.** (1987). Scatter factor is a fibroblast-derived modulator of epithelial cell mobility. *Nature* **327**, 239-242.
- Studer, M., Lumsden, A., ArizaMcNaughton, L., Bradley, A. and Krumlauf, R.** (1996). Altered segmental identity and abnormal migration of motor neurons in mice lacking Hoxb-1. *Nature* **384**, 630-634.
- Tanabe, Y. and Jessell, T. M.** (1996). Diversity and pattern in the developing spinal cord. *Science* **274**, 1115-1123.
- Tanabe, Y., William, C. and Jessell, T. M.** (1998). Specification of motor neuron identity by the MNR2 homeodomain protein. *Cell* **95**, 67-80.
- Taniguchi, M., Yuasa, S., Fujisawa, H., Naruse, I., Saga, S., Mishina, M. and Yagi, T.** (1997). Disruption of semaphorin III/D gene causes severe abnormality in peripheral nerve projection. *Neuron* **19**, 519-530.
- Tessier-Lavigne, M. and C. Goodman.** (1996). The molecular biology of axon guidance. *Science* **274**, 1123-1133.
- Théry, C., Sharpe, M. J., Batley, S. J., Stern, C. J. and Gherardi, E.** (1995). Expression of HGF/SF, HGF1/MSP and c-met suggests new functions during early chick development. *Dev. Genet.* **17**, 90-101.
- Tosney, K. W.** (1991). Cells and cell-interactions that guide motor axons in the developing chick embryo. *BioEssays* **13**, 17-23.
- Tsuchida, T., Ensini, M., Morton, S. B., Baldassare, M., Edlund, T., Jessell, T. M. and Pfaff, S. L.** (1994). Topographic organization of embryonic motor neurons defined by expression of LIM homeobox genes. *Cell* **79**, 957-970.
- Tucker, A., Lumsden, A. and Guthrie, S.** (1996). Cranial motor axons respond differentially to the floor plate and cranial sensory ganglia in collagen gel co-cultures. *Eur. J. Neurosci.* **8**, 906-916.
- Uehara, Y., Minowa, O., Mori, C., Shiota, K., Kuno, J., Noda, T. and Kitamura, N.** (1995). Placental defect and embryonic lethality in mice lacking hepatocyte growth factor/scatter factor. *Nature* **373**, 702-705.
- Varela-Echavarría, A., Pfaff, S. L. and Guthrie, S.** (1996). Differential expression of LIM homeobox genes among motor neuron subpopulations in the developing chick brainstem. *Mol. Cell Neurosci.* **8**, 242-257.
- Varela-Echavarría, A. and Guthrie, S.** (1997). Molecules making waves in axon guidance. *Genes Dev.* **11**, 545-557.
- Varela-Echavarría, A., Tucker, A., Püschel, A. W. and Guthrie, S.** (1997). Motor axon subpopulations respond differentially to the chemorepellents netrin-1 and semaphorin D. *Neuron* **18**, 193-207.
- Wahl, C. M., Noden, D. M. and Baker, R.** (1994). Developmental relations between sixth nerve motor neurons and their targets in the chick embryo. *Dev. Dyn.* **201**, 191-202.
- Yamamoto, Y., Livet, J., Pollock, R. A., Garces, A., Arce, V., de Laypeyrière, O. and Henderson, C. E.** (1997). Hepatocyte Growth Factor (HGF/SF) is a muscle-derived survival factor for a subpopulation of embryonic motoneurons. *Development* **124**, 2903-2913.